

The impact of *in utero* BPA exposure on the development of breast cancer

Undergraduate Research Thesis

Presented in partial fulfillment of the requirements for graduation “with Honors Research Distinction” in the undergraduate colleges of The Ohio State University

By  
Claire Kovalchin

The Ohio State University  
April 2018

Project Advisor: Dr. Craig Burd, Department of Molecular Genetics

## Table of Contents

Abstract.....	3
Introduction.....	4
Materials and Methods.....	7
Results.....	11
Discussion.....	18
Conclusions.....	23
References.....	25
Acknowledgments.....	31

## Abstract

Previous studies have shown that *in utero* exposure to diethylstilbestrol (DES), a synthetic form of estrogen, increases the risk of developing various forms of cancer, including breast cancer, later in life.<sup>1</sup> Bisphenol A (BPA) has been shown to act as a synthetic estrogen, and acts similarly to DES in rodents.<sup>2</sup> Both compounds belong to a class of compounds known as endocrine disrupting compounds (EDCs), known to have hormonal activity. *In utero* BPA exposure can also increase the risk of developing breast cancer in rodents.<sup>3</sup> The exact mechanism by which BPA alters the morphology of the mammary gland to create this susceptibility, however, is unknown. Using immunohistochemistry, we have shown that BPA affects the expression of two key proteins, Ki67 and ER $\alpha$ , in the stroma, correlating to significant defects in the epithelium. These data suggest that BPA induced alterations in the stroma may affect the epithelial phenotype, specifically ductal branching.

One cell type of the stroma, fibroblasts, contribute to the production of the extracellular matrix (ECM), which provides structural support for the epithelial ducts. These cells also communicate with the developing epithelium through secreted proteins. Therefore, fibroblasts are critical to both the structure and function of the mammary gland. Alterations to fibroblasts have the potential to lead to changes that can disrupt normal development and cellular function in the mammary gland. We performed transcriptome analysis and identified the extracellular matrix to be significantly altered in the BPA exposed mammary glands, so collagen deposition was investigated. We demonstrate that BPA exposed fibroblasts have increased collagen in the mammary glands, a molecular phenotype shown to increase cancer risk.

## Introduction

From the 1940s to the 1960s, pregnant women were prescribed diethylstilbestrol (DES), a synthetic estrogen used to reduce the risk of premature delivery or miscarriage.<sup>4</sup> The female children of women who took DES during pregnancy have been found to have an increased risk of developing a myriad of reproductive tract abnormalities, including clear cell adenocarcinoma, endometriosis, and infertility.<sup>1,5</sup> These women, termed “DES daughters”, have also been found to have a two-fold increased risk of developing breast cancer later in life.<sup>1</sup> In rodent models, bisphenol A (BPA) has been shown to act as a synthetic estrogen, like DES.<sup>6</sup> Both compounds belong to a class known as endocrine disrupting compounds (EDCs) which have hormonal activity. It is commonly accepted that exposures to EDCs during the critical periods of embryonic and fetal development are more likely to cause harm than exposure that occurs during adulthood.<sup>7</sup>

BPA is a compound used to make most plastics and resins. It is classified as a high production volume chemical, with releases to the environment currently exceeding one million pounds per year.<sup>8</sup> Humans can be exposed to BPA from canned food and plastic products like water bottles and baby bottles, among many other sources. A study conducted by the Center for Disease Control found that 93% of people over the age of six had a detectable level of BPA in their urine.<sup>9</sup> Furthermore, it has been found in human amniotic fluid, demonstrating that *in utero* BPA exposure is a relevant health concern, and its effects merit further study.<sup>10</sup> In DES daughters, there was a long latency period between *in utero* exposure to DES and the beginning of disease, which was not typically observed until after the age of forty. Therefore, the potential harmful effects from BPA associated with increased plastics usage in the 1980s and 1990s have not yet manifested in the population, provided that there is a long latency period between BPA

exposure and disease, as there is with DES exposure.<sup>11</sup> Breast cancer is the second deadliest cancer in women, and one in eight women will develop breast cancer in her lifetime.<sup>12</sup> It is of the utmost importance that we determine the impact of *in utero* BPA exposure on increasing breast cancer risk and the mechanism of its effects, so that we understand the risk that BPA poses to the population and are better equipped to manage cancer prevention efforts.

*In utero* BPA exposure has already been shown to increase the risk of developing breast cancer in rodents.<sup>3</sup> In mice, exposure has been shown to inhibit development of the mammary gland early in life, then accelerate it later in life.<sup>13-16</sup> The activation of the estrogen receptor (ER) may be implicated in these changes, however, the exact mechanism by which BPA alters the morphology of the developing mammary gland to create this susceptibility is unknown.

Mammary gland development begins on embryonic day (E) 10.5 when the milk line forms, and continues on E11.5 when the placode forms (Figure 1).<sup>17</sup> The placode cells then invaginate into the mesenchyme to form the primordial epithelial bud. The surrounding mesenchyme serves as the only estrogen receptor (ER) -expressing compartment of the embryonic gland.<sup>17-20</sup> Once these developing epithelial buds sink beneath the epidermis starting at E13.5, they remain completely surrounded by the ER-positive mesenchyme until approximately E16.5.<sup>18</sup> The bud then proliferates out of the mesenchyme through the fat pad and into primary rudimental branching.<sup>17</sup> It is unknown whether mammary gland susceptibility to EDCs like BPA varies throughout the different stages of embryonic development. Notably, cancers of the reproductive tract in DES daughters were found to be associated specifically with first trimester exposure to DES, indicating that there may be a critical window for EDC exposure during embryological and fetal development.<sup>1, 21, 22</sup>

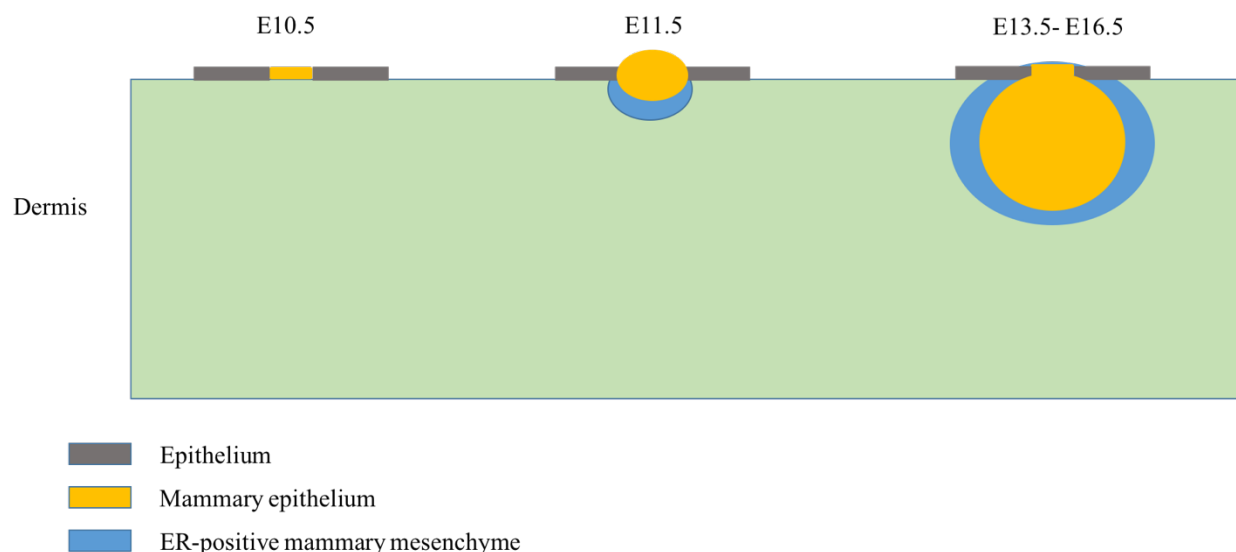


**Figure 1- Murine fetal mammary gland development.** Development of the mammary gland begins around E10.5, and continues when the placode forms on E11.5. The cells then invaginate into the mesenchyme to form the primordial epithelial bud. The surrounding mesenchyme serves as the only estrogen receptor (ER) - expressing compartment of the embryonic gland, and the cells remain completely surrounded by this mesenchyme until E16.5.

One particular component of the stroma, the extracellular matrix, is known to be deregulated in tumors. In addition, alterations in the expression of certain extracellular matrix components have been shown to increase cancer susceptibility.<sup>23</sup> For example, increased collagen deposition within the mammary gland is a phenotype that has been shown to increase cancer risk.<sup>24</sup> BPA exposure has been shown to alter collagen expression within the mammary gland, however, it is unknown whether this relationship is still valid when BPA exposure occurs *in utero*.<sup>25</sup>

We hypothesize that different windows of *in utero* exposure to BPA lead to varying degrees of altered phenotypes within the mammary gland. Specifically, we believe that both morphological changes, such as changes in epithelial elongation, and molecular changes, such as differences in ER expression, will be observed. In addition, we hypothesize that collagen

deposition will be altered in mammary glands exposed to BPA *in utero*, as previous studies have reported differences in collagen deposition when mammary glands are exposed to BPA.<sup>25</sup>

## **Materials and Methods**

### *Fetal Exposure to BPA in the Varied Treatment Model*

Animal experiments were performed in compliance with the protocol approved by The Ohio State University institutional animal care and use committee (protocol number 2013A00000030). Pregnant CD-1 mice were fed a diet containing minimal levels of phytoestrogen (2019X Teklad Rodent Diets; Harlan Laboratories Inc., Indianapolis, IN). The mice received a daily intraperitoneal (IP) injection of BPA, with a dosage of 25 ug per kg of body weight, between embryonic days (E) 8.5 and 18.5, the beginning stages of mammary gland development. E0.5 was defined as the day that a vaginal plug was observed following mating. Vehicle oil was administered to a second cohort during the same time frame, as a control. A variety of different treatment schemes were used during the E8.5-18.5 period, corresponding to embryonic developmental milestones. Mice were treated according to the following treatment schemes: E8.5 to E12.5 (BPA 1), E8.5 to E16.5 (BPA 2), E15.5 to E18.5 (BPA 3), and E8.5 to E18.5 (BPA 4). Mice treated with vehicle oil as the control received IP injections from E8.5 to E18.5 (OIL).

Female pups were separated from males, and then euthanized at 4.5, 14, and 20 weeks of age. Mice from the same litter were divided among different time points to prevent littermates from being used for the same analysis. All mice at least 8 weeks of age were sacrificed during the estrus stage of the estrous cycle, which was initially identified using vaginal cytology, and later confirmed by hematoxylin and eosin analysis of the uterus, ovaries, and vagina. The fourth

inguinal mammary glands were harvested from each mouse. One mammary gland from each mouse was whole mounted and stained with carmine-aluminum. The other gland was embedded in paraffin, sectioned, and used for immunohistochemical analysis.

### *Mammary Whole Mount and Immunohistochemical Analysis*

Carmine-aluminum stained mammary whole mounts were used for morphological analysis. Digital images of whole mounts were obtained using a dissection microscope (Zeiss Stemi SV11 Apt stereomicroscope) at 0.6X magnification, equipped with a camera (AxioCam 506 color) and Zeiss ZEN software. For early-life mammary glands (4.5 weeks of age), epithelial elongation was measured in millimeters plus or minus the distance from a line on the leading edge of the lymph node to the furthest point of epithelial branching. The number of terminal duct ends (TDEs) and the number of terminal end buds (TEBs) were also counted. A width of 0.15mm was used as a threshold for determining qualification for TEBs. The percentage of epithelial area was quantified using color thresholding and selection of epithelial branching in ImageJ.<sup>26</sup> The percentage was used to normalize the number of TEBs counted for each treatment and was represented as a ratio. All measurements were confirmed through blind analysis ( $n \geq 7$ ).

Carmine-aluminum stained whole mounts of mature (14 and 20 weeks of age) mammary glands were also analyzed by determining the percentage of epithelial area using color thresholding and selection in ImageJ.<sup>26</sup> Digital images were obtained using a dissection microscope as described above. Images were captured with one field of view from each biological replicate (age 14 weeks,  $n \geq 9$ ; age 20 weeks,  $n \geq 3$ ) selected from the leading edge of the mammary gland, in front of the lymph node.



Immunohistochemistry (IHC) was used to analyze both early-life and mature mammary glands. Sections were stained using a Bond Rx autostainer (Leica Biosystems, Buffalo Grove, IL) and automated software (Bond Rx, version 4.0) in order to run optimized protocols. The slides were baked at 65°C for 15 minutes, and then dewaxing, rehydration, antigen retrieval, blocking, primary antibody incubation, postprimary antibody incubation, detection [3,30 - diaminobenzidine (DAB) or Bond Polymer Red Detection], and counterstaining using Bond reagents (Leica) were performed by automated software. Samples were then removed from the autostainer, dehydrated, mounted, and coverslipped. Antibodies for the following markers were diluted in antibody diluent (Leica): rabbit antibody  $\alpha$ -smooth muscle actin (SMA; 1:5000; Abcam, Cambridge, UK), ER $\alpha$  (1:2000; E115; GeneTex, Irvine, CA), and Ki67 (1:200, Abcam); and rat antibody cytokeratin 8 (1:2000; TROMA-I-C; Developmental Studies Hybridoma Bank, University of Iowa).

Four field-of-view images were captured for each biological replicate at 20X magnification using the Vectra Automated Multispectral imaging system. TDEs and ducts were imaged for 4.5-week-old mice, while alveolar buds and ducts were imaged for 14-week-old mice. Four images of each type of structure for each biological replicate were acquired. Tissue compartment segmentation and quantification of positivity were performed using InForm Advanced Image Analysis Software, version 2.0.2 (Perkin Elmer, Waltham, MA). The InForm Tissue Finder software was used to determine tissue compartment positivity. Positivity was determined by manually segmenting tissue compartments into the stroma and the epithelium using SMA- positive staining to designate the epithelial compartment, using object-based segmentation to identify positive cells, and scoring using 2-bin positivity to identify the component DAB signal as positive for the staining performed (ER $\alpha$  or Ki67). Scoring was also

used to determine a threshold to differentiate between DAB-positive and DAB-negative, or hematoxylin and eosin only, nuclei. The threshold for positivity was determined separately for both the stroma and the epithelium, and these thresholds were used to score all images. Results are represented as the percentage of positivity normalized to the total area of mammary tissue determined using the Inform software.

### *Transcriptional Profiling*

In order to determine which genes may be altered by *in utero* BPA exposure, and which pathways these genes correspond to, transcriptional profiling was performed. RNA from fibroblasts, luminal epithelial cells, and basal epithelial cells was isolated from the mammary glands of 13-week-old mice treated *in utero* with either oil or BPA as previously described.<sup>27</sup> Libraries for Illumina next generation sequencing were generated and sequenced by the Ohio State Genomics Core. Following RNA-seq, differentially regulated genes were identified and subjected to Ingenuity Pathway Analysis to detect altered processes.

### *Collagen Deposition Analysis*

Pregnant CD-1 mice were cared for as described above, and received a daily intraperitoneal (IP) injection of BPA or vehicle oil, with a dosage of 25 ug per kg of body weight, between E8.5 and 18.5. Female pups were separated from males, and then euthanized at 14 weeks. Mammary glands were harvested, fixed, paraffin-embedded, sectioned, and stained with Picrosirius red (PSR) in order to visualize the collagen within the gland. The slides were baked at 65°C for 10 minutes, deparaffinized, and soaked in a 1:2 dilution of hematoxylin and eosin in PBS for 3 minutes. The slides were then rinsed in deionized water, washed with

ammonia water for one minute, and again rinsed with deionized water. Sirius red (abcam 150681) was added to the tissue, and the tissue was incubated for one hour. The slides were washed twice in acetic acid solution (abcam 150681), dehydrated, and coverslipped. Two field of view images per biological replicate ( $n \geq 11$ ) were taken, one selected from the leading edge of the gland, and one selected from opposite the leading edge of the gland. Images were taken at 4X magnification using a Nikon Eclipse 50i microscope equipped with an Axiocam506 color Zeiss camera and Zeiss Zen Pro software, then cropped to a uniform size and randomized prior to analysis in ImageJ, so as to blind the analysis. The lymph node was removed and the image was color thresholded to determine the total area of the tissue. The image was then again color thresholded to determine the area of epithelial branching. The total area of PSR staining and the intensity of the PSR staining for each digital image was quantified in ImageJ.<sup>26</sup>

## Results

### *BPA exposure during different in utero windows results in varying phenotypes of the early-life mammary gland*

In order to assess the effect of *in utero* BPA exposure during different stages of embryological development, four different dosing schemes were used that correspond to milestones in the embryological development of the mammary gland (Figure 2A). We examined BPA exposure during the period of milk line formation but before bud invagination into the ER-expressing mesenchyme (BPA1, E8.5 to E12.5), the period from milk line formation through bud invagination into the mesenchyme (BPA2, E8.5 to E16.5), the period during which the epithelium begins to extend toward the fat pad until it has begun branching (BPA3, E15.5 to E18.5), and the duration of exposure that resulted in previously reported phenotypes (BPA4, E8.5 to E18.5).<sup>17-20</sup>

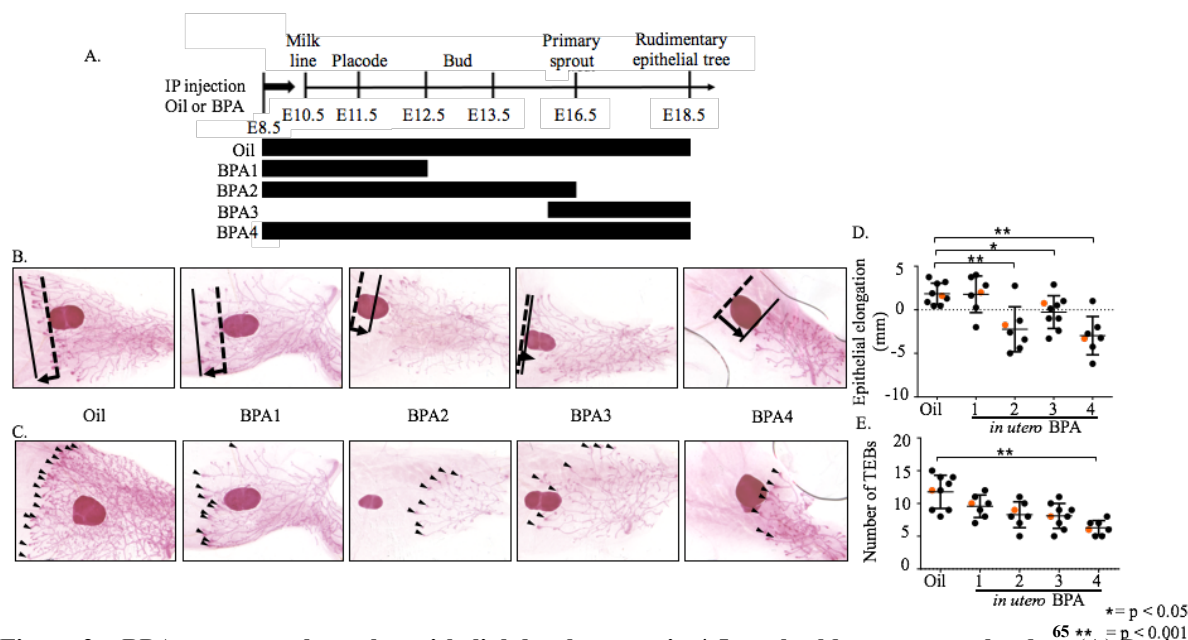


**Figure 2 – BPA exposure alters the epithelial development in 4.5-week-old mammary glands.** (A) Dosing schemes for *in utero* BPA treatments with 25  $\mu\text{g}/\text{kg}\cdot\text{bw}/\text{day}$  BPA, beginning embryonic day (E) 8.5 and varied through 18.5. BPA1: E8.5-12.5; BPA2: E8.5-16.5; BPA3: E15.5-18.5; and BPA4: E8.5-18.5. (B) Carmine-aluminum stained whole mount mammary glands were used to measure epithelial elongation from the leading edge of the lymph node (dashed line) to the most distal portion of the epithelial tree (solid line). Graph represents comparison of epithelial elongation in millimeters, between treatments, and each dot represents separate biological replicates,  $n \geq 7$ . (C) The number of terminal end buds (TEBs, indicated by arrowheads) were counted for each mammary gland. Graph represents comparison of number of TEBs between treatments, each dot representing separate biological replicates,  $n \geq 7$ . Orange dots indicate the data point used for representative images (B) and (C). \* =  $p < 0.05$ , \*\* =  $p < 0.001$ .

By examining carmine-aluminum stained mammary glands from 4.5-week-old mice, we found that the window of *in utero* BPA exposure affected the delayed epithelial growth phenotype that has been previously reported. Specifically, in mice treated with BPA after E12.5, there was a clear defect in epithelial elongation from the leading end of the mammary gland lymph node (Figure 2B, dashed line) to the most distal epithelial branching (Figure 2B, solid line). There was no significant difference between the epithelial elongation in mice treated before E12.5 (BPA1) and the epithelial elongation in control mice. Epithelial elongation for BPA2 ( $P < 0.001$ ) and BPA3 ( $P < 0.05$ ), however, was significantly less than that of the control group and similar to that of mice who were treated with BPA throughout the entirety of fetal mammary gland development (BPA4,  $P < 0.001$ ; Figure 2B;  $n \geq 7$ ). In early-life glands, only

mice who received the BPA4 treatment exhibited a statistically significant reduction ( $P < 0.005$ ) in the number of TDEs (Figure 2C and 2D). While BPA2 and BPA3 did demonstrate decreased numbers of TDEs, this difference was not statistically significant. In addition, recapitulation of the phenotypes observed in previous studies demonstrated an increase in the ratio of TEBS (Figure 2C and 2E) to the total epithelial area in the treatment periods after E12.5 (Figure 2D). Differences at BPA4 reached statistical significance ( $P < 0.005$ ), while the differences at BPA2 and BPA3 demonstrated a phenotypic trend, but were not statistically significant.

ER $\alpha$  expression and proliferation (Ki67) were examined in both the epithelium and the stroma surrounding TDEs and TEBS in 4.5-week-old mice using sections from inguinal mammary gland tissue. To distinguish the epithelial tissue from the surrounding stroma, IHC of SMA was used. The positivity of Ki67 and ER $\alpha$  was determined within both the epithelium and the stroma for each treatment scheme (Figure 3A and 3B,  $n \geq 7$ ). Within the stroma, ER $\alpha$  positivity was significantly increased with BPA 2 ( $P < 0.05$ ), BPA3 ( $P < 0.05$ ), and BPA4 ( $P < 0.001$ ) when compared to controls, while there was no significant difference with BPA1. Ki67 expression, in contrast, was significantly decreased in the stroma surrounding TDEs and TDEs with BPA2 treatment ( $P < 0.001$ ). BPA3 and BPA4 treatments also exhibited a trend in decreased Ki67 positivity, although this trend was not statistically significant (Figure 3B). There were no notable changes in ductal Ki67 positivity in either tissue compartment, across all treatments. Within the epithelium, only BPA4 treatment resulted in significant changes in Ki67 and ER $\alpha$  expression.

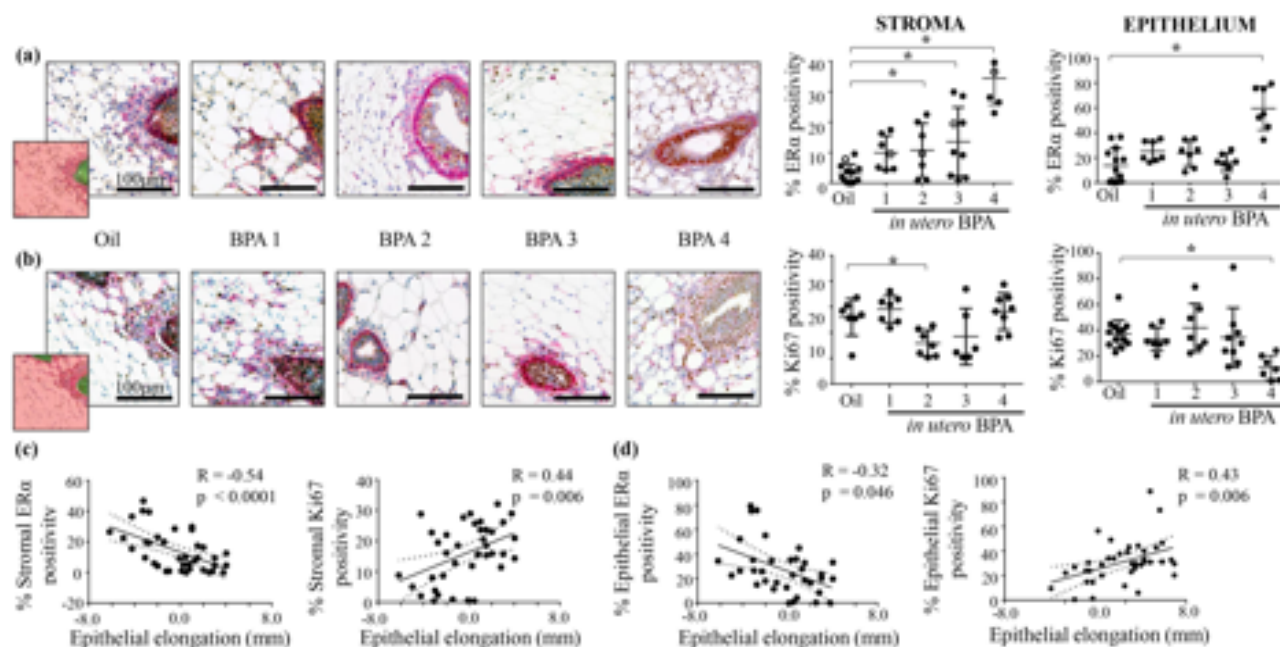


**Figure 3 – Early life epithelial dysfunction of the mammary gland by *in utero* BPA significantly correlates to molecular changes to the stroma.**<sup>65</sup> Mammary glands from 4.5-week-old mice were dual-stained with smooth muscle actin (SMA, pink) and (A) ERα (brown) or (B) Ki67 (brown) (20x magnification); Inset depicts the tissue segmentation of the oil sample by InForm Advanced Image Analysis Software, differentiating the stroma (red) and epithelium (green). Graphs present (A) ERα or (B) Ki67 positivity (%) in the stroma (left), and epithelium (right). Each dot represents separate biological replicates,  $n \geq 7$ . Orange symbols indicate the representative images shown for each treatment. Epithelial elongation (Figure 2B) was correlated to the stromal ERα and Ki67 positivity from matched mammary glands across all treatments. Significant correlations were observed between (C) ERα ( $R^2 = -0.54$ ) and (D) Ki67 positivity (right,  $R^2 = 0.44$ ). \* =  $p < 0.05$ , \*\* =  $p < 0.001$ , \*\*\*\* =  $p < 0.0001$ . Dotted lines indicate 95% confidence interval.

Molecular changes in the stroma (Figure 3C) were found to correlate with early-life dysfunction of epithelial elongation (Figure 2B). When comparing all mammary glands, regardless of the *in utero* exposure window, it was noted that epithelial elongation was correlated significantly and inversely with ERα positivity (Figure 3C, left graph;  $R = -0.54$ ,  $P < 0.0001$ ) and directly with Ki67 positivity (Figure 3C, right graph;  $R = 0.44$ ,  $P < 0.001$ ) within the stroma, even when the BPA4 treatment scheme was excluded. In addition, epithelial elongation significantly correlated with epithelial ERα positivity (Figure 3D, left graph;  $R = -0.32$ ;  $P < 0.05$ ) and Ki67 positivity (Figure 3D, right graph;  $R = 0.43$ ;  $P < 0.05$ ). However, this relationship was only present when BPA4 was included in the analysis.

*BPA exposure during different in utero windows changes ER $\alpha$  expression in the adult mammary gland*

We evaluated both morphological and molecular changes in 14-week-old mice to assess whether early-life defects in the mammary gland translated to later-life development. Dual stained tissue segments revealed that ER $\alpha$  positivity varied between each treatment scheme, most substantially for the epithelial–alveolar structures and surrounding stroma (Figure 4,  $n \geq 4$ ). Similarly to 4.5-week-old mice, 14-week-old mice that received BPA1 treatment exhibited no difference in ER $\alpha$  positivity in either the stroma or the epithelium when compared to control mice. BPA3 treated mice also showed no changes in either tissue compartment when compared with controls. In BPA4 mice, however, ER $\alpha$  positivity was significantly decreased in both the stroma and the epithelium ( $P < 0.05$ ). BPA2 treatment also resulted in a significant decrease in epithelial ER $\alpha$  positivity and a significant difference in stromal ER $\alpha$  positivity (Figure 4). Ki67 positivity was not altered when compared to controls for any treatment, in either tissue compartment (data not shown).

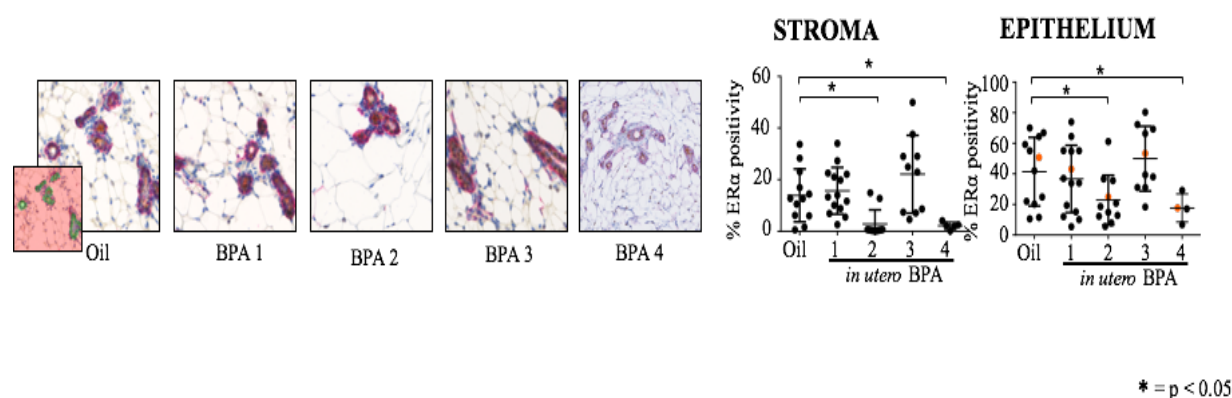


**Figure 4 – ER $\alpha$  expression is altered in the adult mammary gland by *in utero* BPA exposures.**<sup>65</sup>  
Representative images are shown of *in utero*-treated mammary glands from 14-week-old mice dual-stained with SMA and ER $\alpha$ , focused around alveolar structures (20X magnification). The inset depicts the tissue segmentation of the stroma (red) and epithelium (green) in the representative oil-treated gland. Graphs display ER $\alpha$  positivity (%) quantified in the alveolar structures of the epithelium (left) and the surrounding stroma (right). Each dot represents separate biological replicates,  $n \geq 12$ , and orange symbols indicate the representative images shown for each treatment. \* =  $p < 0.05$ , \*\* =  $p < 0.001$ .

*In utero BPA exposure changes the morphology of ducts to varying degrees based on the window of exposure*

Carmine-aluminum stained mammary whole mounts of adult 14-week-old (Figure 5A,  $n \geq 9$ ) and 20-week-old (Figure 5B,  $n \geq 3$ ) mice were examined in order to assess the ability of our model to replicate previous observations that *in utero* BPA exposure increases the epithelial volume and changes ductal morphology. BPA2 and BPA4 mice both exhibited statistically significant increases in epithelial area (Figure 5A,  $P < 0.05$ ), mirroring trends in ER $\alpha$  expression in 14-week-old mice, but no changes were observed in BPA1 and BPA3 treated mice. These phenotypes were consistent through 20 weeks (Figure 5B,  $P < 0.05$ ). While BPA1 and BPA3 treatment showed a trend toward increased epithelial area at 20 weeks, this difference was not statistically significant ( $P = 0.051$  and  $P = 0.082$ , respectively). These data suggest that *in utero* BPA exposure driven alterations that occur during early-life can be propagated into adulthood when exposure occurs after E12.5.

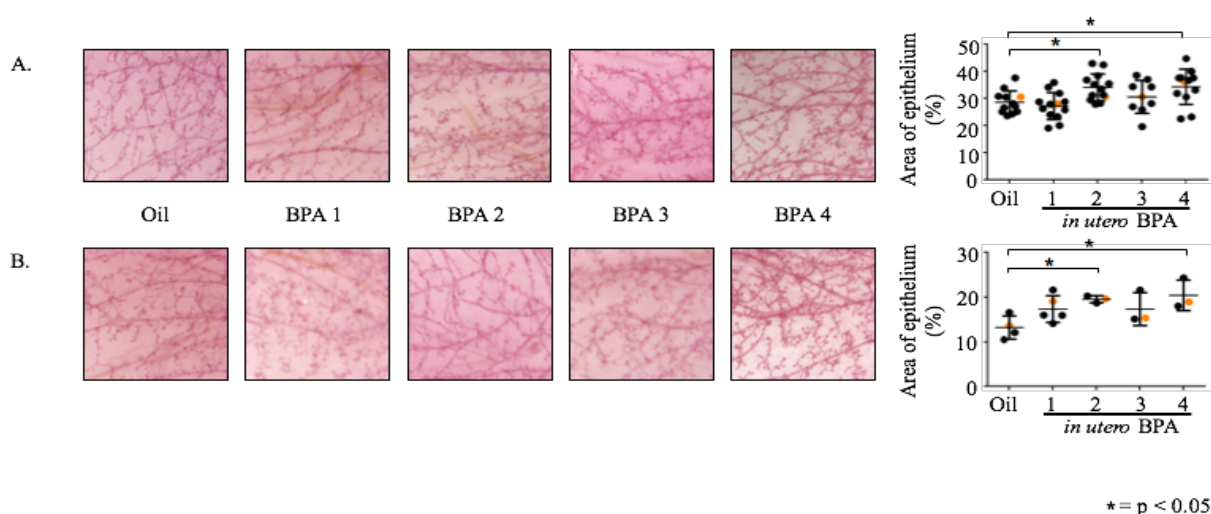


**Figure 5 - *In utero* BPA exposure significantly alters the density and complexity of the epithelium of the mammary gland.**<sup>65</sup> Color thresholding was performed in ImageJ to quantify epithelial area in carmine-stained mammary whole mounts. Representative dissection light microscope images are shown from (A) 14-week-old and (B) 20-week-old adult mice. Graphs represent the area of epithelium as measured by pixels in epithelium out of total pixels in field of view (%). Each dot represents separate biological replicates, (A)  $n \geq 9$  and (B)  $n \geq 3$  and orange symbols indicate the representative mammary gland shown. \* =  $p < 0.05$ .



*In utero BPA exposure alters the extracellular matrix, specifically collagen deposition*

Transcriptional profiling was performed using RNA isolated from fibroblasts, luminal epithelial cells, and basal epithelial cells from 13-week-old mice treated *in utero* with either oil or BPA. It was noted that genes associated with the extracellular matrix were found to be significantly altered in mice that were exposed *in utero* to BPA (Table 1).

Since collagen is a significant component of the extracellular matrix, it was selected for further analysis. Using PSR staining and subsequent analysis in ImageJ, it was determined that in 14-week-old mammary glands that were exposed to *in utero* BPA, both the average area of PSR staining ( $P < 0.005$ ) and the average intensity of PSR staining ( $P < 0.005$ ) were both significantly different from control glands (Figure 6). This indicates that *in utero* BPA exposure alters collagen deposition in adult mammary glands.

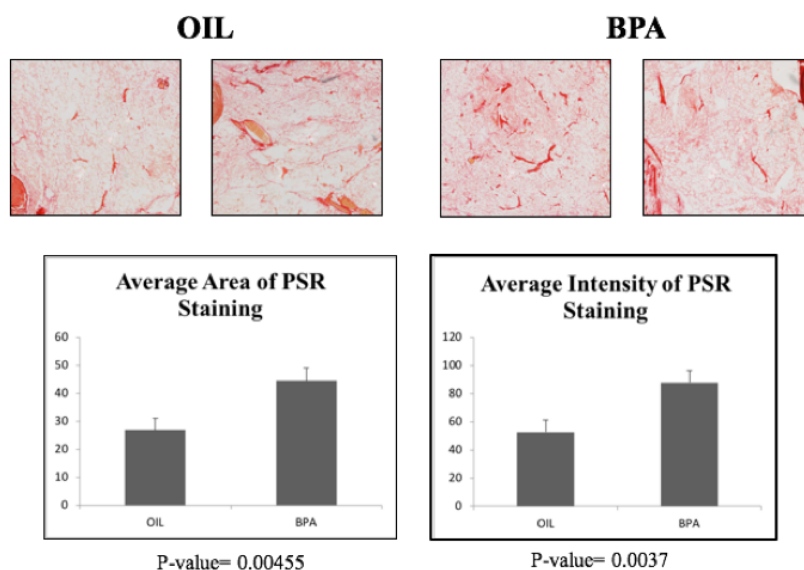


**Figure 6. *In utero* BPA exposure increases collagen in the mammary gland.** Following our *in utero* treatment model, mammary glands from 14-week-old mice were harvested, fixed, paraffin-embedded, sectioned, and stained with Picrosirius red. Two field of view images per biological replicate ( $n \geq 11$ ) were taken, one selected from the leading edge of the gland, and one selected from opposite the leading edge of the gland. Images were taken at 4x magnification using a Nikon Eclipse 50i microscope, cropped, randomized, and analyzed in ImageJ. Images are representative of each treatment's average area of PSR staining and average PSR intensity.

	Luminal epithelial	Basal epithelial/ MaSC	Fibroblast
<b>Molecular functions</b>	(1) Structural molecule activity [1.92E-10] ← (2) Ribosome structure [2.87E-09] (3) Ribosomal binding of rRNA [1.62E-04] (4) PDGF-binding [1.95E-04] (5) ECM structural constituent [3.42E-04] ← (5)	(1) Structural constituent of ribosome [1.47E-31] (2) Structural molecule activity [1.07E-20] (3-5) NADH dehydrogenase (ubiquinol-quinone) activity [3.86E-11] (19)	(1) Heparin binding [1.33E-06] (2) Growth factor binding [3.79E-06] (3) Macromolecule complex binding [4.26E-06] ← (4) ECM structure [1.10E-05] ← (5) Glycosaminoglycan binding [1.22E-05] (23)
<b>Biological processes</b>	(1, 2) Co-translational protein targeting to membrane [3.64E-12, 6.54E-12] (3, 4) Protein targeting to endoplasmic reticulum [7.68E-12, 1.05E-11] (5) non-sense-mediated decay [2.85E-11] (29) Ribosome biogenesis [6.53E-08] (37) Collagen fibril organization [1.02E-06] ← (50) Macromolecule catabolic process [3.07E-05] (62) Collagen catabolic process [2.19E-04] ← (66) ECM organization [3.55E-04] ← (95)	(1-5) Co-translational protein targeting and to the endoplasmic reticulum [6.70E-38, 6.79E-37, 1.27E-36, 4.26E-36, 2.01E-34, 7.01E-34] (10) Translational initiation [2.77E-28] (14) mRNA catabolic process [7.99E-27] (19) Ribosome biogenesis [2.71E-23] (72) Cellular macromolecule catabolic process [1.34E-10] (82) Cellular macromolecule localization [4.12E-09] (103) Inflammatory response [5.43E-04] (115) Fibroblast proliferation [1.66E-03] (128)	(1-5) Cell movement/ migration Locomotion [1.36E-10, 5.79E-10, 4.98E-09, 5.50E-09, 5.50E-09] (10) Morphogenesis of the epithelium [7.67E-08] (12) Collagen metabolic process [9.36E-08] ← (15) Collagen-activated signaling [3.34E-07] (16) Cell adhesion [3.60E-07] (20) Regulation of proliferation [6.19E-07] (28) ECM organization [3.09E-06] ← (321)
<b>Cellular components</b>	(1-5) Cytosolic ribosome [2.12E-11, 4.69E-10, 4.82E-09, 9.40E-07, 1.01E-06] (6-9) banded and fibrillar collagen and collagen trimers [1.01E-06, 2.88E-06, 2.88E-06] ← (17) ECM [9.72E-05] ← (20)	(1-5) Cytosolic ribosome [2.22E-38, 6.72E-33, 2.59E-30, 6.73E-29, 9.48E-24] (21-23) Focal adhesion and junctions [9.27E-12, 1.17E-11, 1.46E-11] (47)	(1-5) ECM organization and components [5.75E-13, 2.95E-12, 2.80E-07, 2.83E-07, 3.09E-07] (12, 13) Banded and fibrillar collagen [5.18E-05] ← (17) Growth factor complex [2.35E-04] (22) Basal lamina [3.96E-04] (37)
<b>Pathways</b>	(1) Peptide chain elongation [3.65E-11] (18) Ribosome [2.12E-09] (28) Assembly of collagen fibrils and other multimeric structures [1.22E-05] ← (30) Translation initiation [1.57E-05] (37) Collagen biosynthesis and enzymes [6.20E-04] ← (38) ECM organization [6.62E-04] ← (46)	(1) Eukaryotic translation elongation [1.14E-41] (2) Peptide chain elongation [1.33E-40] (19) Ribosome [3.24E-33] (41) Gene expression [6.03E-08] (45)	(1, 2) Ensemble of genes encoding ECM [3.65E-14, 1.24E-12] (3, 4) ECM [2.74E-08, 4.16E-07] (5) Genes encoding structural ECM glycoproteins [7.63E-07] (13) PI3K-Akt signaling pathway [1.42E-04] (54)

**Table 1- Transcriptional profiling identifies the extracellular matrix as significantly altered in BPA exposed mammary glands.** RNA from fibroblasts, luminal epithelial cells, and basal epithelial cells was isolated from the mammary glands of 13 week old mice treated *in utero* with either oil or BPA. Following RNA-seq, differentially regulated genes were subjected to Ingenuity Pathway Analysis to identify altered processes. Red arrows highlight processes and components associated with the extracellular matrix.

## Discussion

### *Susceptibility to in utero BPA varies throughout fetal development*

Exposure to EDCs during the critical periods of embryonic and fetal development can effect harmful changes in hormone-dependent organ development that can increase the risk of developing cancer.<sup>7</sup> Exposure during the first trimester was shown to be the most detrimental for DES daughters, who were found to have the greatest risk of developing vaginal cancer when exposure occurred this period.<sup>1, 28, 29</sup> To our knowledge, however, no study has been performed to establish a similar window of susceptibility for breast cancer development. While *in utero* BPA exposure has been shown to increase both the number of TEBs and cancer risk in rodents,

the mechanism by which BPA causes these defects and creates this susceptibility that extends to adulthood is not well understood.<sup>30-32</sup> Therefore, we selected four windows of mammary gland development within which we could test the effects of BPA exposure. We observed that defects within the mammary gland were present when BPA treatment occurred after E12.5, after the epithelial bud had invaginated into the ER $\alpha$ -expressing mesenchyme. BPA1, treatment from E8.5 to E12.5, showed no evidence of mammary gland defects. BPA2 and BPA4 (schemes that included treatment from E12.5 to E18.5) exhibited significant defects, consistent with previous reports. At 4.5 weeks of age, BPA exposure resulted in decreased epithelial elongation, a decreased number of TDEs, and an increase in the ratio of TEBs to the total area of the epithelium (Figure 2B and 2C). BPA1, BPA2, and BPA3 all demonstrated an increase in Ki67 positivity, while BPA4 treatment resulted in a significant decrease in Ki67 positivity when compared with controls. Most of the significant early and later-life phenotypes were observed when the window of exposure included E12.5 to E16.5 (BPA2 to BPA4).

A potential caveat of our treatment model was that BPA2 and BPA4, the windows which resulted in the most significantly altered phenotypes, were treated for longer periods of *in utero* development (8 and 10 days versus 4 and 3 days for BPA1 and BPA3, respectively). Despite this, it is important to note that BPA3, while only treated for 3 embryonic days, resulted in a phenotype that was substantial, but diminished, when compared to controls. In addition, the BPA1 dosing scheme, spanning 4 days, did not result in noticeable defects to the mammary gland, indicating that the total duration of BPA exposure is not the driving factor for the observed changes. It is important to note that due to the rate of clearance of BPA in mice, exposure persists after the defined treatment windows, and therefore, the true exposure period cannot be identified in its entirety.<sup>33</sup> However, the different dosing schemes used did produce

differing mammary gland phenotypes, and exposure that occurred before E12.5 generally did not produce substantial defects.

*The Role of ER $\alpha$  in mammary gland changes caused by in utero BPA exposure*

BPA exposure has been thought to cause deregulated mammary development and later-life defects through its ability to interact with the ERs.<sup>34-39</sup> ER $\alpha$  activation within the stroma has been suggested to be the driver of BPA-induced alterations within the mammary gland.<sup>16,19,40</sup> Notably, BPA-induced changes in murine mammary glands were found to be blocked when mice were treated with the estrogen antagonist fulvestrant, indicating that BPA may act through ERs in the stroma.<sup>41</sup> Taken together with our findings, this suggests that the stroma plays a key role in the development of the mammary epithelium, as previously reported.<sup>42-45</sup> In addition, it also suggests that the stroma is involved in effecting later-life mammary defects. It is possible that the BPA-altered mesenchyme can reprogram the epithelium through paracrine signaling after inappropriate ER $\alpha$  activation. It follows that this signaling would result in the most significantly altered phenotype when the developing mammary gland is completely surrounded by the ER $\alpha$  - positive mesenchyme, which occurs between E12.5 and E16.5.<sup>18</sup> This window is represented by dosing schemes BPA2 and BPA4, which were found to have the most significantly altered phenotypes.

It has been shown previously that in mice, only 4% of stromal cells are weakly ER $\alpha$ -positive in immediate postnatal development; ER $\alpha$  expression continues to increase in both the number of positive cells as well as in intensity throughout adolescence and adulthood.<sup>46</sup> This finding was recapitulated by examining the ER $\alpha$  positivity within the 4.5-week-old control mammary glands. BPA was found to increase the number of ER $\alpha$ -expressing cells in TDEs in 4.5-week-old mice, as demonstrated in BPA4 mice, and in both BPA2 ( $P < 0.05$ ) and BPA4 ( $P <$

0.05), ER $\alpha$  expression was significantly reduced in the epithelium. Until recently, the importance of ER $\alpha$  signaling within the stroma of the mammary gland during development has not been well understood. Recently, it was shown that BPA also interferes with mammary gland development even in an *ex vivo* model which eliminates any effects that BPA could elicit in the hypothalamic–pituitary–gonadal axis, supporting the conclusion that BPA acts upon the ER $\alpha$ -positive stroma to alter mammary gland development.<sup>47</sup>

While BPA has been shown to interact with other hormone receptors, such as ER $\beta$ , studies investigating knockout models of these receptors make it clear that ER $\alpha$  is primarily responsible for later-life development of the mammary gland.<sup>35, 37, 48-52</sup> In addition, BPA2 mice, who exhibited the most highly altered phenotype, were not exposed to BPA during the period in which ER $\beta$  is expressed (E18). Therefore, our model suggests that *in utero*, BPA acts on ER-expressing mesenchymal cells to alter signaling within the mammary gland and cause phenotypical changes. Our model also indicates that ER $\alpha$  activation is crucial for these BPA-induced alterations.

We acknowledge that there may be differences in mammary gland *in utero* ER $\alpha$  expression between humans and mice. For example, humans express ER $\alpha$  beginning after week 30 of gestation, while mice do not express ER $\alpha$  in the epithelium until after birth. In addition, no study has ever demonstrated *in utero* ER $\alpha$  expression in the mesenchyme in humans. Furthermore, the period during which we found the developing mammary gland most susceptible to BPA-induced defects (E12.5 to E16.5) corresponds to weeks 7 through 14 of human gestation, but no study has investigated ER $\alpha$  expression before week twelve, and only a few have done so before week 18.<sup>53-55</sup> Weeks 7 through 14 correspond to the end of the first trimester of human gestation;<sup>46</sup> this is also when the highest rates of vaginal misdifferentiation effects were noted.<sup>1,56</sup>

No study has yet correlated breast cancer susceptibility to the window of exposure, but one study has correlated vaginal defects to breast cancer susceptibility.<sup>1,22</sup> Together, these data suggest that human susceptibility to breast cancer occurs before ER $\alpha$  begins to be expressed in the epithelium in the third trimester.

### *Influence of stromal signaling on mammary gland defects*

The importance of stromal-epithelial interactions within the mammary gland has long been known to play an important role in mammary gland development, and our *in utero* BPA exposure model provides further support for this relationship.<sup>42-44, 57</sup> Even when ER is not expressed, estrogenic compounds can still act directly on mammary tissue to alter the development of the epithelium.<sup>41</sup> In addition, disruption of the communication that occurs between the stroma and the epithelium can result in tumorigenesis.<sup>44, 57-62</sup> Therefore, determining the effects of BPA exposure on this process is necessary to elucidating the mechanism through which BPA creates cancer susceptibility. A significantly higher number of ER $\alpha$ -positive stromal cells surround the TDEs in early-life mammary glands exposed *in utero* to BPA (Figure 3A). This observation could suggest that these mammary glands are undergoing puberty prematurely, since the number of ER $\alpha$ -positive stromal cells has been shown to increase during puberty.<sup>46,63</sup> In addition, it has been previously demonstrated that stromal ER $\alpha$  staining is confined to only undifferentiated mesenchymal cells, rather than to adipocytes or fibroblasts.<sup>63</sup> This suggests that *in utero* BPA exposure can cause an increase in undifferentiated mesenchymal cells, which can promote tumor growth and metastasis. It follows that BPA may stimulate the development of the epithelium indirectly through ER $\alpha$ -positive progenitors in the stroma.<sup>14, 16, 59, 64, 65</sup>

### *The effects of BPA on collagen deposition*

Collagen accounts for a significant component of the extracellular matrix and is important for maintaining the structure of tissue. Using PSR staining, we demonstrate that *in utero* BPA exposure results in an increase in the amount of collagen within the mammary gland. It is known that increased collagen within the mammary gland, causing denser breast tissue, is correlated with an increased risk of breast cancer. The tumor microenvironment, which includes the extracellular matrix, is involved in tumor progression, and tumors are often characterized by the remodeling and stiffening of the extracellular matrix.<sup>23</sup> Furthermore, increased collagen expression and deposition have previously been shown to be implicated in tumor progression, especially in mammary tumors.<sup>24</sup> Therefore, the increase in mammary gland collagen deposition that we found to be caused by *in utero* BPA exposure is significant because this is a phenotype that has been shown to increase cancer risk.

### **Conclusion**

Despite the absence of ER $\alpha$  positivity within the epithelium of BPA-exposed mammary glands, significant epithelial effects were observed following our treatment model. These alterations in the morphology of the mammary gland were noted when *in utero* exposure occurred between E12.5 and E16.5 (BPA2 and BPA4 treatment windows). This demonstrates that the timing of *in utero* exposure can influence cancer risk later in life. Similar changes were noted in women exposed to DES *in utero*, who were found to have a twofold increased risk of developing breast cancer after the age of 40.<sup>1, 21, 22</sup> Notably, women with vaginal epithelium changes found to be associated with first trimester DES exposure had a higher risk of breast cancer.<sup>1, 22</sup> In humans, the mammary bud begins to invade the parenchyma during week of eight

of gestation, during the first trimester, and this corresponds to E12.5 in the gestation of mice.<sup>46</sup>

The period of development beginning at E12.5 was observed to be when the mammary gland was most susceptible to BPA-induced defects; these defects were observed in both early and later life mice. This data suggests that ER $\alpha$  may play a role in mediating BPA-induced alterations in the mammary gland.

We also demonstrate that *in utero* BPA exposure causes increased collagen deposition in the mammary gland, a molecular phenotype shown to increase cancer risk, indicating that BPA exposure alters the extracellular matrix, a crucial component of the mammary gland.<sup>24</sup> It is commonly accepted that high breast density is correlated with an increased incidence of breast cancer. Together, our data demonstrate the need to further characterize the role of ER $\alpha$  in *in utero* BPA caused mammary gland defects and to further investigate potential defects in the extracellular matrix.



## References

1. Hoover RN et al. (2011). Adverse Health Outcomes in Women Exposed *In Utero* to Diethylstilbestrol. *N Engl J Med*, 365(14):1304-1314.
2. Schönfelder G et al. (2004). Developmental Effects of Prenatal Exposure to Bisphenol A on the Uterus of Rat Offspring. *Neoplasia*, 6(5):584–594.
3. Durando M et al. (2007). Prenatal bisphenol A exposure induces preneoplastic lesions in the mammary gland in Wistar rats. *Environ Health Perspect*, 115(1):80-6.
4. Diethylstilbestrol (DES) and Cancer. National Cancer Institute, 2011. Accessed from [www.cancer.gov/about-cancer/causes-prevention/risk/hormones/des-fact-sheet](http://www.cancer.gov/about-cancer/causes-prevention/risk/hormones/des-fact-sheet)
5. Wei M et al. (2016). Effects of Prenatal Environmental Exposures on the Development of Endometriosis in Female Offspring. *Reprod Sci*, 23(9):1129-38.
6. Rubin BS. (2011). Bisphenol A: an endocrine disruptor with widespread exposure and multiple effects. *J Steroid Biochem Mol Biol*, 127(1-2):27-34.
7. Holborn T, vom Saal FS, Soto AM. (1993). Developmental Effects of Endocrine-Disrupting Chemicals in Wildlife and Humans. *Environ Health Perspect*, 101(5):378-84.
8. Bisphenol A Action Plan. U.S. Environmental Protection Agency, 2010. Accessed from [www.epa.gov](http://www.epa.gov)
9. Calafat AM et al. (2008). Exposure of the U.S. population to bisphenol A and 4-tertiary-octylphenol: 2003-2004. *Environ Health Perspect*, 116(1):39-44.
10. Balakrishnan B et al. (2010). Transfer of bisphenol A across the human placenta. *Am J Obstet Gynecol*, 202(4):393.e1-7.
11. World Plastic Production 1950-2015. Plastics Europe: Association of Plastics Manufacturers, 2016. Accessed from <https://committee.iso.org/files/live/sites/tc61/files/The%20Plastic%20Industry%20Berlin%20Aug%202016%20-%20Copy.pdf>
12. Cancer Statistics Center. American Cancer Society, 2017. Accessed from [www.cancerstatisticscenter.cancer.org/](http://www.cancerstatisticscenter.cancer.org/)
13. Macon MB, Fenton SE. (2013). Endocrine disruptors and the breast: early life effects and later life disease. *J Mammary Gland Biol Neoplasia*, 18(1):43–61.
14. Markey CM, Luque EH, Munoz De Toro M, Sonnenschein C, Soto AM. (2001). In utero exposure to bisphenol A alters the development and tissue organization of the mouse mammary gland. *Biol Reprod*, 65(4):1215–1223.

15. Mori T, Bern HA, Mills KT, Young PN. (1976). Long-term effects of neonatal steroid exposure on mammary gland development and tumorigenesis in mice. *J Natl Cancer Inst*, 57(5):1057–1062.
16. Vandenberg LN, Maffini MV, Schaeberle CM, Ucci AA, Sonnenschein C, Rubin BS, Soto AM. (2008). Perinatal exposure to the xenoestrogen bisphenol-A induces mammary intraductal hyperplasias in adult CD-1 mice. *Reprod Toxicol*. 26(3-4):210–219.
17. Robinson GW, Karpf AB, Kratochwil K. (1999). Regulation of mammary gland development by tissue interaction. *J Mammary Gland Biol Neoplasia*, 4(1):9–19.
18. Robinson GW. (2007). Cooperation of signalling pathways in embryonic mammary gland development. *Nat Rev Genet*, 8(12):963–972.
19. Wadia PR, Cabaton NJ, Borrero MD, Rubin BS, Sonnenschein C, Shioda T, Soto AM. (2013). Low-dose BPA exposure alters the mesenchymal and epithelial transcriptomes of the mouse fetal mammary gland. *PLoS One*, 8(5):e63902.
20. Lemmen JG, Broekhof JL, Kuiper GG, Gustafsson JA, van der Saag PT, van der Burg B. (1999). Expression of estrogen receptor alpha and beta during mouse embryogenesis. *Mech Dev*, 81(1-2):163–167.
21. Hatch EE, Palmer JR, Titus-Ernstoff L, Noller KL, Kaufman RH, Mittendorf R, Robboy SJ, Hyer M, Cowan CM, Adam E, Colton T, Hartge P, Hoover RN. (1998). Cancer risk in women exposed to diethylstilbestrol in utero. *JAMA*, 280(7):630–634.
22. Palmer JR, Wise LA, Hatch EE, Troisi R, Titus-Ernstoff L, Strohshnitter W, Kaufman R, Herbst AL, Noller KL, Hyer M, Hoover RN. (2006). Prenatal diethylstilbestrol exposure and risk of breast cancer. *Cancer Epidemiol Biomarkers Prev*, 15(8): 1509–1514.
23. Schedin P, Keely PJ. (2011). Mammary gland ECM remodeling, stiffness, and mechanosignaling in normal development and tumor progression. *Cold Spring Harb Perspect Biol* 3(1):a003228.
24. Fang M, Yuan J, Peng C, Li Y. (2014). Collagen as a double-edged sword in tumor progression. *Tumour Biol* 35(4):2871-82.
25. Betancourt AM, Mobley JA, Russo J, Lamartiniere CA. (2010). Proteomic analysis in mammary glands of rat offspring exposed in utero to bisphenol A. *J Proteomics* 73(6): 1241-53.
26. Abramoff MD, Magalhaes PJ, Ram SJ. (2004). Image processing with Image J. *Biophotonics Int*. 11(7):36–42.

27. Kendrick H, Regan JL, Magnay FA, Grigoriadis A, Mitsopoulos C, Zvelebil M, Smalley MJ. (2008). Transcriptome analysis of mammary epithelial subpopulations identifies novel determinants of lineage commitment and cell fate. *BMC Genomics* 9:591,2164-9-591.
28. Adam E, Decker DG, Herbst AL, Noller KL, Tilley BC, Townsend DE. (1977). Vaginal and cervical cancers and other abnormalities associated with exposure in utero to diethylstilbestrol and related synthetic hormones. *Cancer Res*, 37(4):1249–1251
29. Herbst AL, Ulfelder H, Poskanzer DC. (1971). Adenocarcinoma of the vagina. Association of maternal stilbestrol therapy with tumor appearance in young women. *N Engl J Med.*, 284(15):878–881.
30. Ninomiya K, Kawaguchi H, Souda M, Taguchi S, Funato M, Umekita Y, Yoshida H. (2007). Effects of neonatally administered diethylstilbestrol on induction of mammary carcinomas induced by 7, 12-dimethylbenz(a)anthracene in female rats. *Toxicol Pathol*, 35(6):813–818.
31. Kawaguchi H, Miyoshi N, Miyamoto Y, Souda M, Umekita Y, Yasuda N, Yoshida H. (2009). Effects of fetal exposure to diethylstilbestrol on mammary tumorigenesis in rats. *J Vet Med Sci*, 71(12): 1599–1608.
32. Yoshikawa T, Kawaguchi H, Umekita Y, Souda M, Gejima K, Kawashima H, Nagata R, Yoshida H. (2008). Effects of neonatally administered low-dose diethylstilbestrol on the induction of mammary carcinomas and dysplasias induced by 7,12-dimethylbenz [a] anthracene in female rats. *In Vivo*, 22(2):207–213.
33. Pottenger LH, Domoradzki JY, Markham DA, Hansen SC, Cagen SZ, Waechter JM Jr. (2000). The relative bioavailability and metabolism of bisphenol A in rats is dependent upon the route of administration. *Toxicol Sci*, 54(1):3–18.
34. Hong EJ, Park SH, Choi KC, Leung PC, Jeung EB. (2006). Identification of estrogen-regulated genes by microarray analysis of the uterus of immature rats exposed to endocrine disrupting chemicals. *Reprod Biol Endocrinol*, 4:49. 8.
35. Li Y, Burns KA, Arao Y, Luh CJ, Korach KS. (2012). Differential estrogenic actions of endocrine-disrupting chemicals bisphenol A, bisphenol AF, and zearalenone through estrogen receptor  $\alpha$  and  $\beta$  in vitro. *Environ Health Perspect*, 120(7):1029–1035.
36. Prossnitz ER, Barton M. The G-protein-coupled estrogen receptor GPER in health and disease. (2011). *Nat Rev Endocrinol*. 7(12):715–726.
37. Matsushima A, Liu X, Okada H, Shimohigashi M, Shimohigashi Y. (2010). Bisphenol AF is a full agonist for the estrogen receptor ER $\alpha$  but a highly specific antagonist for ER $\beta$ . *Environ Health Perspect*. 118(9):1267–1272.

38. Gertz J, Reddy TE, Varley KE, Garabedian MJ, Myers RM. (2012). Genistein and bisphenol A exposure cause estrogen receptor 1 to bind thousands of sites in a cell type-specific manner. *Genome Res*, 22(11):2153–2162.
39. Blair RM, Fang H, Branham WS, Hass BS, Dial SL, Moland CL, Tong W, Shi L, Perkins R, Sheehan DM. (2000). The estrogen receptor relative binding affinities of 188 natural and xenochemicals: structural diversity of ligands. *Toxicol Sci*, 54(1):138–153.
40. Saji S, Jensen EV, Nilsson S, Rylander T, Warner M, Gustafsson JA. (2000). Estrogen receptors alpha and beta in the rodent mammary gland. *Proc Natl Acad Sci USA*, 97(1): 337–342.
41. Speroni L, Voutilainen M, Mikkola ML, Klager SA, Schaeberle CM, Sonnenschein C, Soto AM. (2017). New insights into fetal mammary gland morphogenesis: differential effects of natural and environmental estrogens. *Sci Rep*, 7:40806.
42. Sakakura T. (1987). *Mammary Embryogenesis*. New York: Plenum Press; doi: 10.1007/978-1-4899-5043-7\_2
43. Sakakura T. (1991). New aspects of stroma-parenchyma relations in mammary gland differentiation. *Int Rev Cytol*, 125:165–202. 71.
44. Parmar H, Cunha GR. (2004). Epithelial–stromal interactions in the mouse and human mammary gland in vivo. *Endocr Relat Cancer*, 11(3):437–458. 72.
45. Maffini MV, Calabro JM, Soto AM, Sonnenschein C. (2005). Stromal regulation of neoplastic development: age-dependent normalization of neoplastic mammary cells by mammary stroma. *Am J Pathol*, 167(5):1405–1410
46. Hovey RC, Trott JF, Vonderhaar BK. (2002). Establishing a framework for the functional mammary gland: from endocrinology to morphology. *J Mammary Gland Biol Neoplasia*, 7(1):17–38.
47. Giesbrecht GF, Ejaredar M, Liu J, et al. (2017). Prenatal bisphenol a exposure and dysregulation of infant hypothalamic-pituitary-adrenal axis function: findings from the APrON cohort study. *Environmental Health*, 16:47. doi:10.1186/s12940-017-0259-8.
48. Kurosawa T, Hiroi H, Tsutsumi O, Ishikawa T, Osuga Y, Fujiwara T, Inoue S, Muramatsu M, Momoeda M, Taketani Y. (2002). The activity of bisphenol A depends on both the estrogen receptor subtype and the cell type. *Endocr J*. 49(4):465–471.
49. Korach KS, Couse JF, Curtis SW, Washburn TF, Lindzey J, Kimbro KS, Eddy EM, Migliaccio S, Snedeker SM, Lubahn DB, Schomberg DW, Smith EP. (1996). Estrogen receptor gene disruption: molecular characterization and experimental and clinical phenotypes. *Recent Prog Horm Res*, 51:159–186.

50. Kregge JH, Hodgins JB, Couse JF, Enmark E, Warner M, Mahler JF, Sar M, Korach KS, Gustafsson JA, Smithies O. (1998). Generation and reproductive phenotypes of mice lacking estrogen receptor beta. *Proc Natl Acad Sci USA*, 95(26):15677–15682.
51. Couse JF, Korach KS. (1999). Estrogen receptor null mice: what have we learned and where will they lead us? *Endocr Rev*, 20(3):358–417.
52. Mallepell S, Krust A, Chambon P, Briskin C. (2006). Paracrine signaling through the epithelial estrogen receptor alpha is required for proliferation and morphogenesis in the mammary gland. *Proc Natl Acad Sci USA*, 103(7):2196–2201.
53. Keeling JW, Ozer E, King G, Walker F. (2000). Oestrogen receptor alpha in female fetal, infant, and child mammary tissue. *J Pathol*, 191(4):449–451.
54. Naccarato AG, Viacava P, Vignati S, Fanelli G, Bonadio AG, Montruccoli G, Bevilacqua G. (2000). Bio-morphological events in the development of the human female mammary gland from fetal age to puberty. *Virchows Arch*, 436(5):431–438.
55. Friedrichs N, Steiner S, Buettner R, Knoepfle G. (2007). Immunohistochemical expression patterns of AP2alpha and AP2gamma in the developing fetal human breast. *Histopathology*, 51(6):814–823.
56. Noller KL, Decker DG, Lanier AP, Kurland LT. (1972). Clear-cell adenocarcinoma of the cervix after maternal treatment with synthetic estrogens. *Mayo Clin Proc*, 47(9):629–630.
57. Shekhar MP, Werdell J, Santner SJ, Pauley RJ, Tait L. (2001). Breast stroma plays a dominant regulatory role in breast epithelial growth and differentiation: implications for tumor development and progression. *Cancer Res*, 61(4):1320–1326.
58. Donjacour AA, Cunha GR. (1991). Stromal regulation of epithelial function. *Cancer Treat Res*, 53:335–364.
59. Cunha GR, Bigsby RM, Cooke PS, Sugimura Y. (1985). Stromal–epithelial interactions in adult organs. *Cell Differ*, 17(3):137–148.
60. Farber E. (1984). The multistep nature of cancer development. *Cancer Res*, 44(10):4217–4223.
61. van den Hooff A. (1988). Stromal involvement in malignant growth. *Adv Cancer Res*, 50:159–196.
62. Barcellos-Hoff MH. (2001). It takes a tissue to make a tumor: epigenetics, cancer and the microenvironment. *J Mammary Gland Biol Neoplasia*, 6(2):213–221.
63. Haslam SZ, Nummy KA. (1992). The ontogeny and cellular distribution of estrogen receptors in normal mouse mammary gland. *J Steroid Biochem Mol Biol*, 42(6):589–595.

64. Mu~noz-de-Toro M, Markey CM, Wadia PR, Luque EH, Rubin BS, Sonnenschein C, Soto AM. (2005). Perinatal exposure to bisphenol-A alters peripubertal mammary gland development in mice. *Endocrinology*, 146(9):4138–4147
65. Shyamala G, Ferenczy A. (1984). Mammary fat pad may be a potential site for initiation of estrogen action in normal mouse mammary glands. *Endocrinology*, 115(3):1078–1081.
66. Hindman AR, Mo XM, Helber HL, Kovalchin CE, Ravichandran N, Murphy AR, Fagan AM, St John PM, Burd CJ. (2017). Varying susceptibility of the female mammary gland to in utero windows of BPA exposure. *Endocrinology* 158(10):3435-47.

**Acknowledgments**

Dr. Craig Burd, for serving as my advisor and providing guidance and mentorship throughout the project, as well as for providing feedback on my written thesis and oral presentation.

Andrea Hindman, Corinne Haines, and Clarissa Wormsbaeher for their immeasurable support, teaching, and mentorship.

Dr. Gina Sizemore and Dr. Harald Vaessin, for providing their time and expertise.

The sponsors of the Mayers Summer Research Scholarship, for providing funding for this project.